Chemical Oxidative Degradation of Acridine Orange Dye in Aqueous Solution by Fenton's Reagent

Chiing-Chang Chen[a] (陳錦章), Ren-Jang Wu[b] (吳仁彰),
Yi-You Tzeng[b] (曾乙祐) and Chung-Shin Lu[c]* (盧長興)
[a]*Department of Science Application and Dissemination, National Taichung University, Taichung 403, Taiwan, R.O.C.*
[b]*Department of Applied Chemistry, Providence University, Taichung 433, Taiwan, R.O.C.*
[c]*Department of General Education, National Taichung Nursing College, Taichung 403, Taiwan, R.O.C.*

Degradation of acridine orange (AO) in aqueous solution by Fenton's reagent (Fe^{2+} and H_2O_2) was investigated. The effects of different reaction parameters such as initial AO concentration, pH value of solution, ferrous concentration, hydrogen peroxide concentration, and the presence of chloride ion on the oxidative degradation of AO were investigated. Under optimum conditions, 2 mM H_2O_2, 0.4 mM Fe^{2+} and pH 3.0, the initial 0.2 mM AO solution was reduced by 95.8% within 10 min. The primary intermediates of the degradation reaction of AO were identified. The analytical results indicated that the *N*-de-methylation degradation of AO dye took place in a stepwise manner to yield mono-, di-, tri-, and tetra-*N*-de-methylated AO species generated during the Fenton process. The probable degradation pathways were proposed and discussed.

Keywords: Fenton's reagent; Acridine orange; Hydroxyl radical; *N*-de-methylation.

INTRODUCTION

Acridine orange (AO) is a heterocyclic dye containing nitrogen atoms which is widely used in the fields of printing and dyeing, leather, printing ink, and lithography.[1] It has also been used extensively in biological stains. Toxicological investigations indicate that aminoacridine has mutagenic potential.[2] The release of this colored wastewater in the ecosystem is a dramatic source of water pollution, eutrophication, and perturbation in aquatic life.[3] Therefore, a method of treating the wastewater containing AO is highly desirable now and in the near future.

Conventional wastewater treatment methods such as precipitation, adsorption, air stripping, flocculation, reverse osmosis, and ultrafiltration can be used for color removal from dye-contaminated effluents.[4] However, these methods are non-destructive, since they only transfer the contamination from one phase to another, causing secondary pollution and requiring further treatment. Biological treatment is highly effective for the removal of most contaminants. Despite their success and cost effectiveness, biodegradation processes are inherently slow, do not allow for high degrees of removal, and are not suitable for compounds that are toxic for the microorganisms. The disposal of sludge formed during biological treatment can create additional expenses and environmental problems.[5]

In recent years "advanced oxidation processes" (AOPs) have emerged as an alternative to conventional methods. AOPs are based on the generation of very reactive species such as hydroxyl radicals, which oxidize a broad range of organic pollutants quickly and non-selectively.[6] Among the various AOPs that have been developed the application of Fenton's reagent for the destruction of water contaminants is one of the promising technologies because of its powerful oxidizing potential and comparatively low cost.[7] Fenton oxidation is achieved from the reaction between H_2O_2 and a ferrous salt under acidic conditions according to the following reaction:[8,9]

$$Fe^{2+} + H_2O_2 \rightarrow Fe^{3+} + OH^- + \bullet OH \quad (1)$$

Because of their high oxidation power, hydroxyl radicals are capable of oxidizing many organic pollutants to lower molecular weight compounds and eventually can lead to the complete mineralization, converting them to

* Corresponding author. Tel: +886-4-2219-6999; Fax: +886-4-2219-4990; E-mail: cslu6@ntcnc.edu.tw

CO_2, H_2O and inorganic ions.[10] Fenton's reagent is an attractive oxidative system for wastewater treatment due to the fact that iron is an abundant and non-toxic element, and because hydrogen peroxide is easy to handle and can be broken down to environmentally benign products.[11]

The main objective of this study is to analyze the feasibility of degradation of AO by the Fenton process. The influence of different operational parameters (pH of solution, H_2O_2, Fe^{2+}, AO concentration and the presence of chloride ion) which affect the efficiency of the Fenton reaction in AO oxidation was investigated. Accordingly, identification of the reaction intermediates was performed using HPLC coupled with a photodiode array detector and electrospray ionization mass spectrometer, which reveals the degradation pathways of AO dye in the Fenton process, and can in turn serve as a foundation for future applications.

EXPERIMENTAL

Materials

The acridine orange dye was obtained from Sigma-Aldrich and used without further purification. The chemical structure of the AO dye is shown in Fig. 1. Stock solution containing 10 mM of AO dye in water was prepared, protected from light, and stored at 4 °C. HPLC analysis was employed to confirm the presence of the AO dye as a pure organic compound. Ferrous sulfate and hydrogen peroxide (purity, 30%) were obtained from Acros Organics. $FeSO_4$ solution (100 mM) was prepared and stored at 4 °C for 1 week at most. Reagent-grade ammonium acetate, sodium hydroxide, nitric acid, and HPLC-grade methanol were purchased from Merck. De-ionized water was used throughout this study. The water was purified with a Milli-Q water ion-exchange system (Millipore Co.) to give a resistivity of 1.8×10^7 Ω-cm.

Experimental procedure and analytical methods

The reactions were carried out in a well stirred, batch reactor with a total volume of 100 mL. The oxidation experiments were performed in darkness and at 25 ± 1 °C. Reaction mixtures were obtained by taking an appropriate amount of AO stock solution, adding ferrous sulfate, and adjusting the pH value with nitric acid. The reactions were initiated by adding calculated amounts of hydrogen peroxide. During the experiment, samples were collected after various reaction times and immediately quenched by adding 10 μL of 1 N $Na_2S_2O_3$ solution to the reaction mixtures.

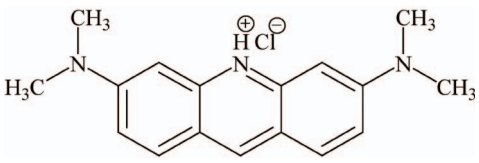

Fig. 1. Chemical structure of acridine orange.

The degradation efficiency of the Fenton process was evaluated using a double beam UV/vis spectrometer (Lambda 25, Perkin-Elmer). The maximum absorbance wavelength (λmax) of AO was found at 492 nm. Throughout the reaction process, the degradation products were never found to interfere with the measurement of AO concentration. Therefore, the concentration of AO in the reaction mixture at different reaction times was determined by measuring the absorption intensity of solution at 492 nm and using a calibration curve. Prior to the measurement, a calibration curve was obtained by using the standard AO solution with known concentrations.

A Waters ZQ LC/MS system–equipped with a binary pump, a photodiode array detector, an autosampler, and a micromass detector–was used for separation and identification. Two different kinds of solvents were prepared in this study. Solvent A was 25 mM aqueous ammonium acetate buffer (pH 6.9) while solvent B was methanol. LC was carried out on an Atlantis™ dC_{18} column (250 mm × 4.6 mm i.d., dp = 5 μm). The flow rate of the mobile phase was set at 1.0 mL/min. A linear gradient was run as follows: t = 0, A = 95, B = 5; t = 20, A = 50, B = 50; t = 35-40, A = 10, B = 90; t = 45, A = 95, B = 5. The column effluent was introduced into the ESI source of the mass spectrometer. Equipped with an ESI interface, the quadruple mass spectrometer with heated nebulizer probe at 350 °C was used with an ion source temperature of 120 °C. ESI was carried out with the vaporizer at 300 °C, nitrogen as sheath (80 psi), and auxiliary (20 psi) gas to assist with the preliminary nebulization and initiate the ionization process. A discharge current of 5 μA was applied. Tube lens and capillary voltages were optimized for the maximum response during perfusion of the AO standard.

The mineralization of AO was monitored by measuring the total organic carbon (TOC) content with a Dohrmann Phoenix 8000 Carbon Analyzer, which employs a u.v./persulfate oxidation method by directly injecting the aqueous solution. For the TOC measurements, potassium phthalate solution was used as the calibration standard with the concentrations of 0, 5, 10, 15, 20 and 25 mg/L.

RESULTS AND DISCUSSION

Effect of initial pH on the decolorization of AO

The effect of the initial pH value of solutions on the decolorization of AO by the Fenton oxidation process was studied in the pH range of 2.0-6.0, and the results are shown in Fig. 2. The results indicated that the decolorization of AO was significantly influenced by the pH of the solution, and the best decolorization efficiency was obtained at pH 3.0. The lower efficiency at high pH values may be due to the precipitation of $Fe(OH)_3$. In this form, iron decomposes H_2O_2 into oxygen and water,[12] and consequently the oxidation rate decreases because less hydroxyl radicals are available. The precipitation of $Fe(OH)_3$ is experimentally confirmed by the presence of turbidity in the experimental samples carried out at pH 5~6.

When the initial pH fell from 6.0 to 3.0, the decolorization efficiency of AO within 60 min increased significantly from 56.3% to 93.2%. However, the decolorization efficiency of AO slowed down to 44.4% with a further decrease of the initial pH from 3.0 to 2.0. This could be explained by the formation of oxonium ion (i.e. $H_3O_2^+$), which enhanced the stability of H_2O_2 and restricted the generation of •OH at low pH conditions (pH < 3.0).[13,14] In addition, the scavenging of •OH by the excess of H^+ is another reason for the lower decolorization efficiency of AO at pH 2.0.[15,16] Thus, 3.0 is recommended as a suitable initial pH for the decolorization of AO by the Fenton oxidation process.

Effect of H_2O_2 dosage on the decolorization of AO

H_2O_2 plays a very important role as a source of •OH generation in the Fenton reaction. It was discovered that if only Fe^{2+} were added in the solution instead of H_2O_2, AO did not show decomposition. The decolorization efficiency increased from 57.1 to 93.2% as a consequence of increasing the H_2O_2 dosage from 0.5 to 2.0 mM at 60 min (Fig. 3). This can be explained by the effect of •OH radicals produced additionally. However, when the dosage rose above 2.0 mM, the decolorization of AO was not improved but dropped. This could be due to the fact that hydroperoxyl radicals (•OOH) were generated in the presence of excess of H_2O_2. Although •OOH is an effective oxidant itself, its oxidation potential is much lower than that of •OH.[17] The hydroperoxyl radicals are much less reactive and do not contribute to the oxidative degradation of organic substrates, which occur only by reaction with •OH.[18] From the experimental results, therefore, 2.0 mM was selected as a suitable H_2O_2 dosage.

Effect of Fe^{2+} dosage on the decolorization of AO

Because H_2O_2, with an oxidation potential of 1.77 eV, has less oxidizing power,[19] AO cannot be effectively oxidized by only adding H_2O_2 to the solution alone. Fe^{2+} is another main parameter in the Fenton reaction that catalytically decomposes H_2O_2 to generate •OH. To study the effect of Fe^{2+} dosage on the decolorization of AO by Fenton oxidation, a series of experiments were conducted with different initial concentrations which ranged from 0.05 to 0.5 mM, and the results obtained are presented in Fig. 4. The results indicated that the decolorization efficiency of AO increased with the increase of the initial concentration of Fe^{2+} in the solution. It can be seen that the decolorization

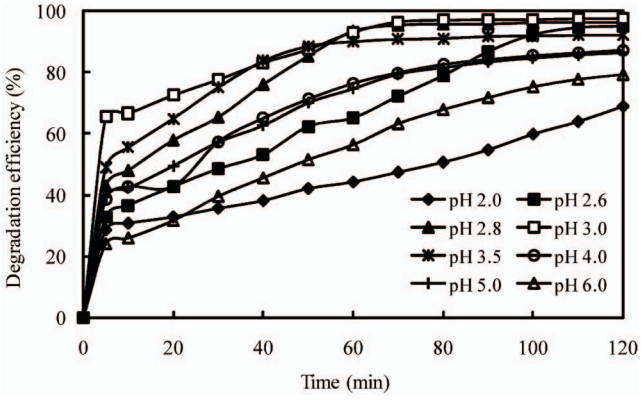

Fig. 2. Effect of initial pH values on the decolorization of AO by Fenton oxidation. Experimental conditions: [AO] = 0.2 mM; [H_2O_2] = 2.0 mM; [Fe^{2+}] = 0.2 mM.

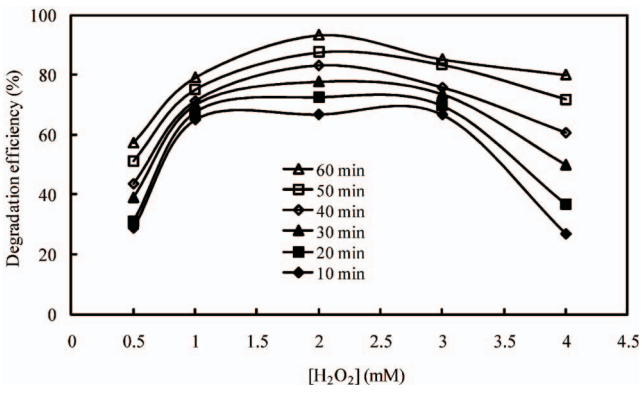

Fig. 3. Effect of H_2O_2 dosage on the decolorization of AO by Fenton oxidation. Experimental conditions: [AO] = 0.2 mM; [Fe^{2+}] = 0.2 mM; pH = 3.0.

was limited at 0.05 mM of Fe^{2+}, and only 15.6% of AO was degraded within 60 min of reaction. In the presence of 0.1, 0.2, 0.3, 0.4 and 0.5 mM of Fe^{2+}, a great improvement of the decolorization of AO could be observed, and the decolorization efficiencies within 60 min of reaction achieved were 76.6%, 93.2%, 97.9%, 98.3% and 98.4%, respectively. The fact that higher decolorization efficiency was achieved at high Fe^{2+} dosages was mainly attributable to the higher production of •OH with more Fe^{2+} in the Fenton reaction.[13]

Effect of AO concentration on the decolorization of AO

It is important from an application point of view to study the dependence of decolorization efficiency on the initial concentration of the AO dye. The decolorization of different concentration of AO was studied, and the results are shown in Fig. 5. It can be seen that the decolorization efficiency of AO fell as AO concentration rose. As AO concentration increased from 0.1 to 1.0 mM, the decolorization efficiency of AO within 60 min of reaction fell from 98.6% to 19.0%. This is because a relatively lower concentration of •OH results from the increasing concentration of AO while the dosage of H_2O_2 and Fe^{2+} remains the same, which leads to a decreasing of the decolorization efficiency of AO.

Several investigators have found that the Fenton reaction for dye degradation follows pseudo-first-order kinetics.[20,21] Regression analysis based on the pseudo-first-order reaction kinetics for the decolorization of AO in Fenton oxidation process was conducted and the results were shown in Table 1. Degradation rate constants, k_{app} (in min^{-1}), were determined from the slope of $\ln(C_0/C) = k_{app}t$ plots, where C_0 and C are the concentration of AO at times 0 and t. As illustrated in Table 1, the degradation rate constants increased with decreasing initial concentrations, indicating a faster reaction rate at lower initial concentration.

Table 1. Kinetic parameters (rate constants and linear regression coefficients R^2) for Fenton oxidation of acridine orange at various initial concentrations

Initial concentration (M)	k_{app} (min^{-1})	R^2
4.0×10^{-4}	0.0113	0.990
6.0×10^{-4}	0.0052	0.942
1.0×10^{-3}	0.0031	0.917

Effect of chloride ion on the decolorization of AO

Salts (sodium chloride, specifically) are important in using many types of dyes, and they co-exist with dyes in the effluent, a fact which could affect the treatment of wastewater.[13] In the presence of inorganic ions the rate for the reaction of H_2O_2 with ferrous ion is different.[22] In our study, the effect of the presence of chloride ion (0.05 to 0.25 M) on the decolorization of AO was investigated, and the results are shown in Fig. 6. It can be seen that chloride ion had a negative impact on the decolorization of AO by Fenton oxidation. The decolorization efficiency within 60 min of reaction decreased from 93.2% to 35.1% as a consequence of increasing the concentration of chloride ions from 0 to 0.25 M, and therefore about 58% of the decolorization efficiency was lost. The inhibitive effect of chloride ions on the decolorization of AO can be explained by

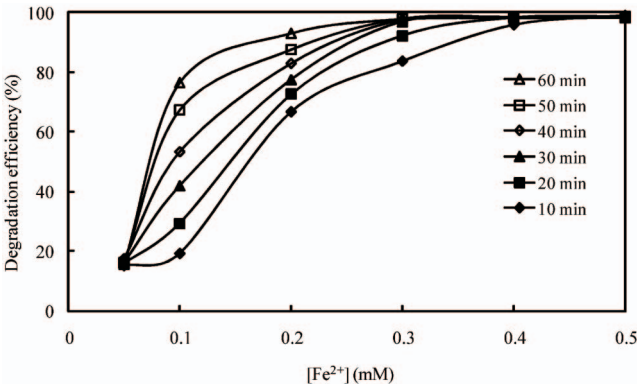

Fig. 4. Effect of Fe^{2+} dosage on the decolorization of AO by Fenton oxidation. Experimental conditions: [AO] = 0.2 mM; [H_2O_2] = 2.0 mM; pH = 3.0.

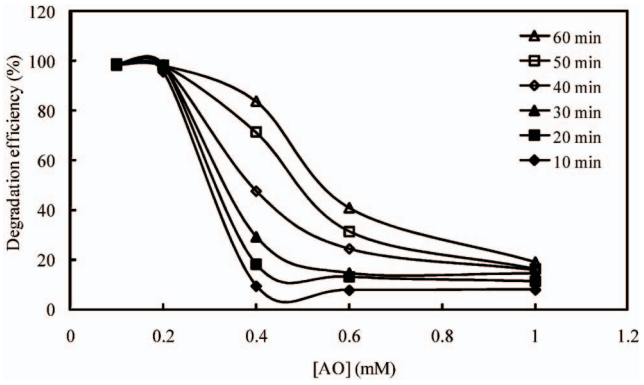

Fig. 5. Effect of AO concentration on the decolorization of AO by Fenton oxidation. Experimental conditions: [H_2O_2] = 2.0 mM; [Fe^{2+}] = 0.4 mM; pH = 3.0.

the scavenging effect of chloride ion on •OH, and the chemical reactions are shown below (Eq. (2) and Eq. (3)).[13,23]

$$Cl^- + {}^{\bullet}OH \rightarrow ClOH^{\bullet -} \quad (2)$$

$$ClOH^{\bullet -} + Fe^{2+} \rightarrow Cl^- + OH^- + Fe^{3+} \quad (3)$$

Mineralization study

In order to assess the degree of mineralization reached during AOPs, the decrease in total organic carbon (TOC) is generally estimated. To investigate the mineralization degree of AO in the Fenton process, the experiments of AO degradation were conducted at an initial AO concentration of 0.2 mM, and the results are shown in Fig. 7. As could be seen, AO degradation is much higher than TOC removal in the Fenton process. Complete mineralization of AO was not achieved after 6 h of oxidation although AO disappeared after 20 min. The great difference between degradation efficiency and mineralization efficiency implied that the products of AO oxidation mostly stayed at the intermediate product stage under the present experimental conditions.

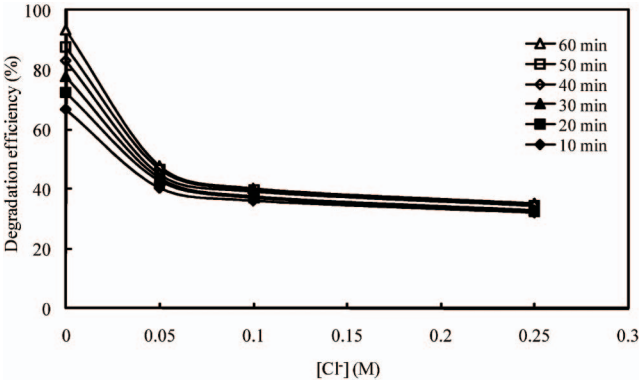

Fig. 6. Effect of chloride ion on the decolorization of AO by Fenton oxidation. Experimental conditions: [AO] = 0.2 mM; $[H_2O_2]$ = 2.0 mM; $[Fe^{2+}]$ = 0.2 mM; pH = 3.0.

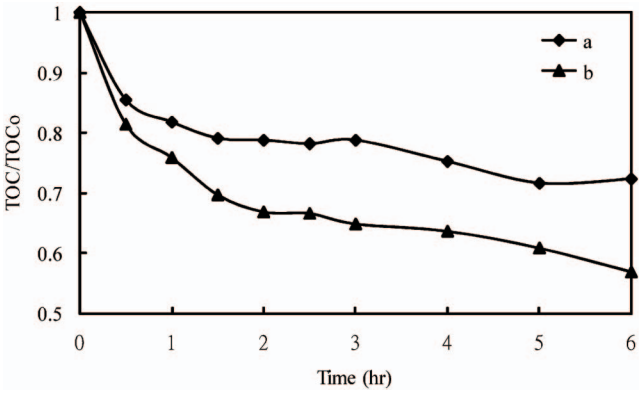

Fig. 7. Depletion in TOC measured as a function of reaction time for an aqueous solution of AO (0.2 mM) in the Fenton process. Experimental conditions: (a) $[H_2O_2]$ = 2.0 mM, $[Fe^{2+}]$ = 0.4 mM, pH = 3.0; (b) $[H_2O_2]$ = 20 mM, $[Fe^{2+}]$ = 2.0 mM, pH = 3.0.

Separation and identification of the intermediates

In order to understand the degradation pathway of the dye during the Fenton process, we identified the intermediates of the degradation of AO with HPLC, coupled with a photodiode array detector and electrospray ionization mass spectrometer. Fig. 8 displays the chromatogram of the reacted solution after 30 min of reaction. At least six compounds were identified at retention times of less than 45 min. One of the peaks was the initial AO; the other five new peaks were those of the intermediates formed. We denoted the AO dye and its related intermediates as species I-VI. Except for the initial AO dye (peak I), the intensities of the other peaks increased at first and subsequently decreased, indicating the formation and transformation of the intermediates.

Fig. 9 displays the absorption spectra of each intermediate in the visible spectral region formed after 30 min of reaction. The absorption spectra of intermediate products were recorded from 200 to 700 nm using a HPLC equipped with a photodiode array detector. In order to compare the maximum absorbance wavelength (λmax) of the spectral bands, the absorption spectra of intermediate products were overlapped and adjusted into the similar absorbance. The absorption maximum of the spectral bands shifts hypsochromically from 489.1 (Fig. 9, Spectrum I) to 458.7 nm (Fig. 9, Spectrum VI). This hypsochromic shift of the absorption band was presumed to result from the stepwise formation of a series of *N*-de-methylated intermediates (i.e., methyl groups were removed one by one as confirmed

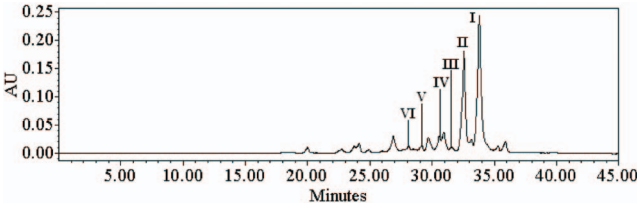

Fig. 8. HPLC chromatogram of the reacted solution after 30 min of Fenton reaction.

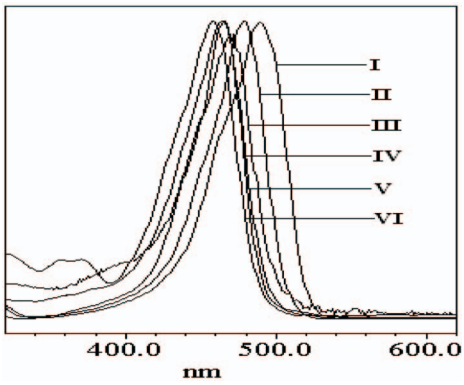

Fig. 9. Absorption spectra of the *N*-de-methylated intermediates formed during the Fenton process of the AO dye corresponding to the peaks in the HPLC chromatogram of Fig. 8. Spectra were recorded using the photodiode array detector. Spectra are denoted I-VI and correspond to the peaks I-VI in Fig. 8, respectively.

by the gradual peak wavelength shifts toward the blue region). The *N*-de-methylation of the AO has the wavelength position of its major absorption band moved toward the blue region, λ_{max}, AO, 489.1 nm; AO-M, 478.2 nm; AO-MM, 472.1 nm; AO-D, 466.0 nm; AO-DM, 464.8 nm; AO-DD, 458.7 nm.

The *N*-de-methylated intermediates were further identified using the HPLC-ESI-MS, and the relevant mass spectra are illustrated in Fig. 10. The molecular ion peaks appeared to be in the acid forms of the intermediates. From the results of mass spectral analysis, we confirmed that the component I, *m/z* = 266.05, in liquid chromatogram was AO (Fig. 10, mass spectra AO). The other components were II, *m/z* = 252.07, *N*-de-mono-methyl-Acridine Orange (Fig. 10, mass spectra AO-M); III, *m/z* = 238.00, *N*,*N*′-de-dimethyl-Acridine Orange (Fig. 10, mass spectra AO-MM); IV, *m/z* = 238.08, *N*,*N*-de-dimethyl-Acridine Orange (Fig. 10, mass spectra AO-D); V, *m/z* = 224.03, *N*,*N*,*N*′-de-trimethyl-Acridine Orange (Fig. 10, mass spectra AO-DM); and VI, *m/z* = 210.00, *N*,*N*,*N*′,*N*′-de-tetramethyl-Acridine Orange (Fig. 10, mass spectra AO-DD).

Table 2 presents the absorption maximum and the mass peaks of the *N*-de-methylated intermediates and the corresponding compounds identified by interpretation of their mass spectra. Two species had protonated molecules of *m/z* = 238 eluted at retention times of 30.95 min (compound IV) and 31.60 min (compound III) during LC/MS, suggesting the formation of di-*N*-de-methylated products of AO. Both intermediates display similar HPLC-ESI-MS characteristics. One of them, AO-MM, was formed by the removal of a methyl group from two different amino groups of the AO molecule. Loosening two methyl groups from the same amino group of the AO dye produced the other one, AO-D. The LC chromatogram revealed a shorter retention time for compound IV than for compound III, suggesting compound IV was more polar. Considering that the polarity of the AO-D species is greater than that of the AO-MM intermediate, we expected the latter to be eluted after the AO-D species. As well, to the extent that two *N*-methyl groups are stronger auxochromic moieties than the *N*,*N*-dimethyl or amino groups are, the maximal absorption of the AO-D intermediate was anticipated to occur at a wavelength shorter than the band position of the AO-MM species.

Degradation pathways of AO dye in the Fenton process

Fenton's reagent is a mixture of hydrogen peroxide and ferrous salt. Hydrogen peroxide decomposes catalytically in the presence of ferrous ions and generates radicals such as the hydroxyl (•OH) and hydroperoxyl (•OOH) radicals.[24] In the process, the major oxidant was the •OH, since

Table 2. Identification of the *N*-de-methylation intermediates of the AO dye by HPLC-ESI-MS

HPLC Peaks	*N*-de-methylation intermediates	Abbreviation	ESI-MS peaks (*m/z*)	Absorption maximum (nm)
I	Acridine Orange	AO	266.05	489.1
II	*N*-de-mono-methyl-Acridine Orange	AO-M	252.07	478.2
III	*N*,*N*′-de-dimethyl-Acridine Orange	AO-MM	238.00	472.1
IV	*N*,*N*-de-dimethyl-Acridine Orange	AO-D	238.08	466.0
V	*N*,*N*,*N*′-de-trimethyl-Acridine Orange	AO-DM	224.03	464.8
VI	*N*,*N*,*N*′,*N*′-de-tetramethyl-Acridine Orange	AO-DD	210.00	458.7

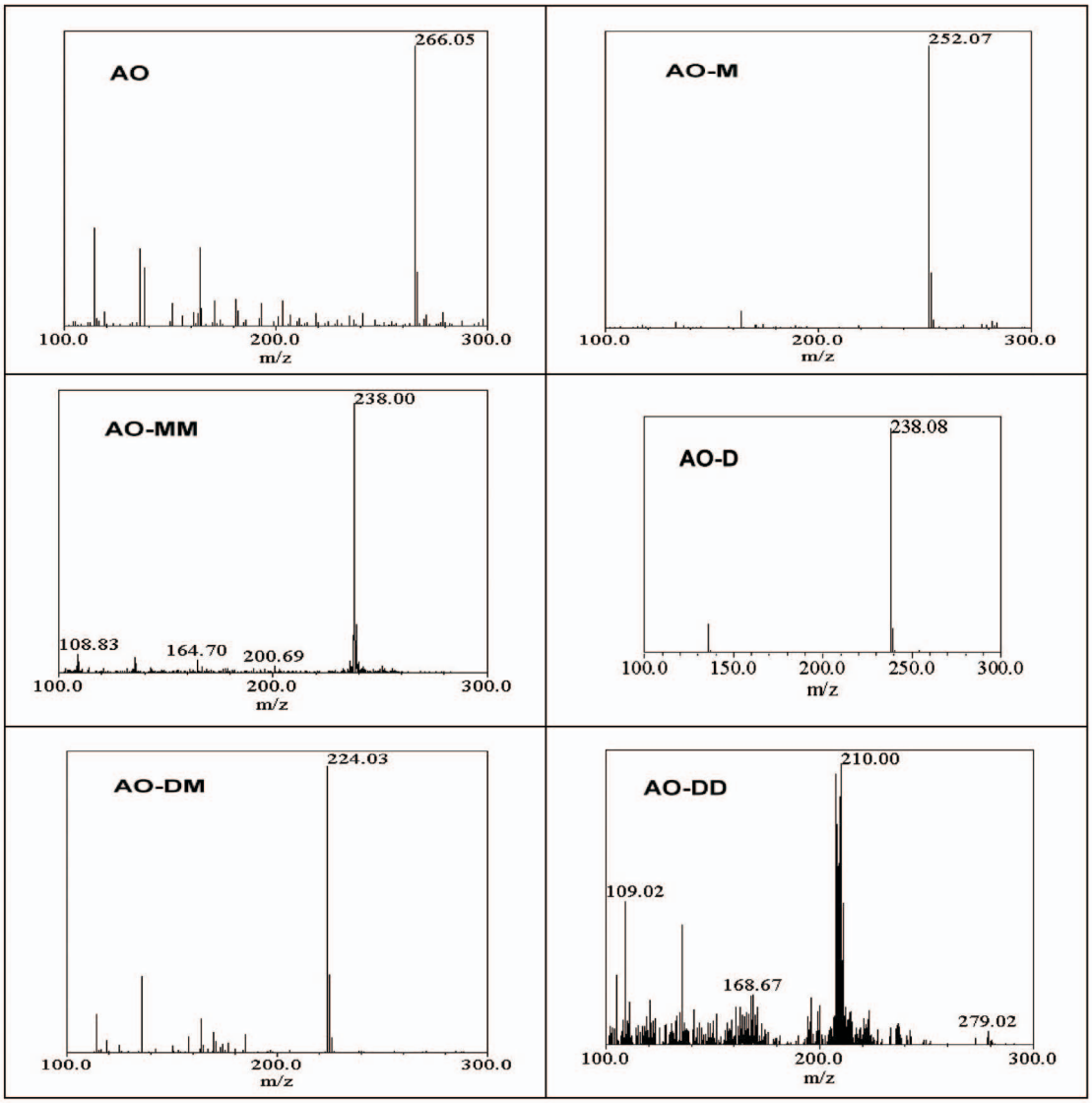

Fig. 10. ESI mass spectra of the *N*-de-methylated intermediates formed during the Fenton process of the AO dye after they were separated by HPLC-ESI-MS method.

•OOH and its conjugate base O_2• were much less reactive as hydroxyl radicals.[25,26]

The *N*-de-methylation of the AO occurs mostly by the attack of the $^{\bullet}$OH species on the *N*,*N*-dimethyl groups of the AO, as shown in Scheme I. Hydroxyl radicals yield carbon-centered radicals upon the H-atom abstraction from the methyl group, or they react with the lone-pair electron on the N atom to generate cationic radicals, which subsequently convert into carbon-centered radicals.[27] The carbon-centered radicals react rapidly with O_2 to produce peroxy radicals that subsequently transform into alkoxy radicals through the bimolecular Russell mechanism.[28] The fragmentation of the alkoxy radical produces a de-methylated product. The mono-de-methylated species, AO-M, can also be attacked by $^{\bullet}$OH species and be implicated in other similar events (H-atom abstraction, oxygen attack, and the bimolecular Russell mechanism) to yield the bi-de-methylated intermediates, AO-MM and AO-D. The *N*-de-methylation process as described above continues until formation of the completely *N*-de-methylated species, AO-DD. The mechanism of AO degradation by TiO_2 photocatalysis was discussed in our previous study.[29] The mechanism of the Fenton process, generating $^{\bullet}$OH radical to oxidize organic compounds, is similar to that of TiO_2 photo-

Scheme I A proposed reaction pathway for acridine orange degradation in acidic aqueous medium in the Fenton process

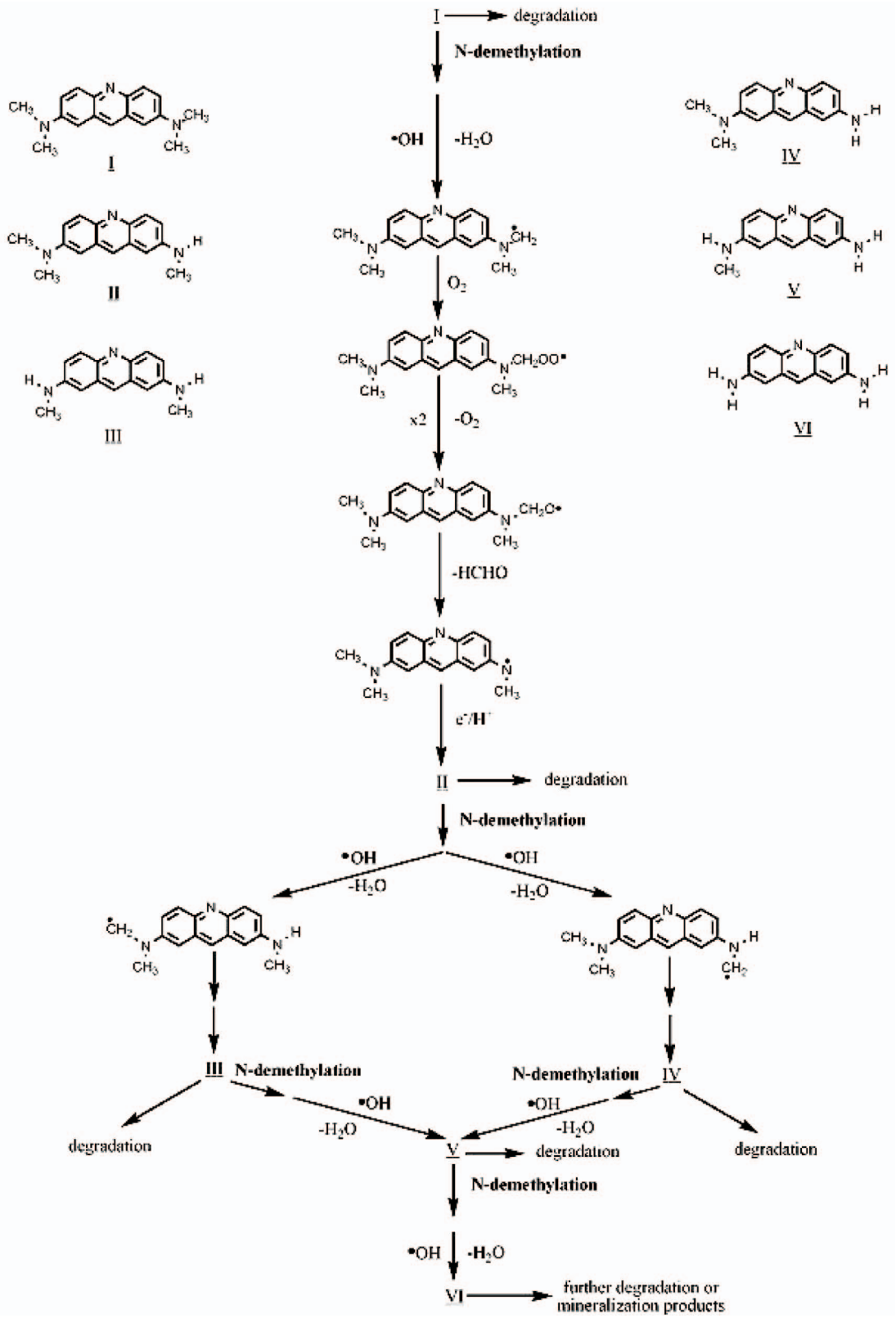

catalysis.

CONCLUSIONS

The Fenton process appears to have the capacity to completely decolourize and partially mineralize the acridine orange dye in aqueous solution in a short reaction time. A direct influence of initial pH on the decolorization of AO could be observed, and the best efficiency was obtained at pH of 3.0. At a constant AO concentration (0.2 mM), decolorization efficiency increased with increasing H_2O_2 and Fe^{2+} concentrations up to a certain level above which decolorization efficiency decreased due to the scavenging effects of H_2O_2 on hydroxyl radicals. A suitable operating condition for the Fenton oxidation of AO was selected as: $[H_2O_2] = 2.0$ mM, $[Fe^{2+}] = 0.4$ mM and pH = 3.0. In the given conditions, more than 95.8% of decolorization efficiency was achieved within 10 min of reaction. However, low TOC removal or mineralization yield and high AO removal indicated the formation of intermediate products. The *N*-de-methylation degradation of the AO dye takes place in a stepwise manner with the various *N*-demethylated intermediate AO species. The methyl groups are removed one by one as confirmed by the gradual wavelength shifts of the maximum-peaks toward the blue region. The process continues until formation of the completely *N*-de-methylated dye.

ACKNOWLEDGMENT

This work was supported by NSC 97-2113-M-438-001 of the National Science Council of the Republic of China.

Received June 25, 2009.

REFERENCES

1. Xie, Y.; Chen, F.; He, J.; Zhao, J.; Wang, H. *J. Photochem. Photobiol. A: Chem.* **2000**, *136*, 235.
2. Brinker, C. J.; Cornils, B.; Bonet, M. *Ullmann's Encyclopedia of Industrial Chemistry, Part A27; Triarylmethane and Diarylmethane Dyes*; 6th ed.; Wiley-VCH: New York, 2001.
3. Faisal, M.; Tariq, M. A.; Muneer, M. *Dyes Pigm.* **2007**, *72*, 233.
4. Kansal, S. K.; Singh, M.; Sud, D. *J. Hazard. Mater.* **2007**, *141*, 581.
5. Guo, J.; Al-Dahhan, M. *Ind. Eng. Chem. Res.* **2003**, *42*, 2450.
6. Daneshvar, N.; Salari, D.; Khataee, A. R. *J. Photochem. Photobiol. A: Chem.* **2004**, *162*, 317.
7. Goi, A.; Veressinina, Y.; Trapido, M. *Chem. Eng. J.* **2008**, *143*, 1.
8. Yoon, J.; Lee, Y.; Kim, S. *Water Sci. Technol.* **2001**, *44*, 15.
9. Neyens, E.; Baeyens, J. *J. Hazard. Mater.* **2003**, *98*, 33.
10. Rizzo, L.; Lofrano, G.; Grassi, M.; Belgiorno, V. *Sep. Purif. Technol.* **2008**, *63*, 648.
11. Papic, S.; Vujevic, D.; Koprivanac, N.; Sinko, D. *J. Hazard. Mater.* **2009**, *164*, 1137.
12. Szpyrkowicz, L.; Juzzolino, C.; Kaul, S. N. *Water Res.* **2001**, *35*, 2129.
13. Sun, S. P.; Li, C. J.; Sun, J. H.; Shi, S. H.; Fan, M. H.; Zhou, Q. *J. Hazard. Mater.* **2009**, *161*, 1052.
14. Kwon, B. G.; Lee, D. S.; Kang, N.; Yoon, J. *Water Res.* **1999**, *33*, 2110.
15. Deng, Y.; Englehardt, J. D. *Water Res.* **2006**, *40*, 3683.
16. Feng, J.; Hu, X.; Yue, P. L.; Zhu, H. Y.; Lu, G. Q. *Ind. Eng. Chem. Res.* **2003**, *42*, 2058.
17. Hameed, B. H.; Lee, T. W. *J. Hazard. Mater.* **2009**, *164*, 468.
18. Neamtu, M.; Zaharia, C.; Catrinescu, C.; Yediler, A.; Macoveanu, M.; Kettrup, A. *Appl. Catal. B: Environ.* **2004**, *48*, 287.
19. Xu, X. R.; Zhao, Z. Y.; Li, X. Y.; Gu, J. D. *Chemosphere* **2004**, *55*, 73.
20. Swaminathan, K.; Sandhya, S.; Sophia, A. C.; Pachhade, K.; Subrahmanyam, Y. V. *Chemosphere* **2003**, *50*, 619.
21. Wang, S. *Dyes Pigm.* **2008**, *76*, 714.
22. Siedlecka, E. M.; Wieckowska, A.; Stepnowski, P. *J. Hazard. Mater.* **2007**, *147*, 497.
23. Ashraf, S. S.; Rauf, M. A.; Alhadrami, S. *Dyes Pigm.* **2006**, *69*, 74.
24. Chan, K. H.; Chu, W. *J. Hazard. Mater.* **2005**, *118*, 227.
25. Bielski, B. H. J.; Cabelli, D. E.; Arudi, R. L. *J. Phy. Chem. Ref. Data* **1985**, *14*, 1041.
26. Frimer, A. A.; Simiuc, M. G. et al. *Oxygen Radicals in Biology and Medicine*; Plenum Press: New York, 1988; pp 29-38.
27. Lee, J.; Choi, W. *Environ. Sci. Technol.* **2004**, *38*, 4026.
28. Russell, G. A. *J. Am. Chem. Soc.* **1957**, *79*, 3871.
29. Lu, C. S.; Mai, F. D.; Wu, C. W.; Wu, R. J.; Chen, C. C. *Dyes Pigm.* **2008**, *76*, 706.